IEEE Access
Multidisciplinary : Rapid Review : Open Access Journal

Received July 20, 2019, accepted September 30, 2019, date of publication October 7, 2019, date of current version October 16, 2019.

Digital Object Identifier 10.1109/ACCESS.2019.2945786

Impact of the Measurement Errors on Synchrophasor-Based WAMS Applications

JIECHENG ZHAO[1], (Member, IEEE), JIN TAN[1], (Member, IEEE), LING WU[1], (Member, IEEE), LINGWEI ZHAN[1], (Member, IEEE), WENXUAN YAO[1], (Member, IEEE), AND YILU LIU[1,2], (Fellow, IEEE)

[1]Department of Electrical Engineering and Computer Science, The University of Tennessee, Knoxville, TN 37996, USA
[2]Oak Ridge National Laboratory, Oak Ridge, TN 37831, USA

Corresponding author: Jiecheng Zhao (jzhao27@vols.utk.edu)

This work was supported in part by the Office of Electricity through the DOE under Contract DE-AC05-00OR22725, in part by the Engineering Research Center Program of the National Science Foundation and the Department of Energy (DOE) through NSF under Award EEC-1041877, and in part by the CURENT Industry Partnership Program.

ABSTRACT Data from Phasor Measurement Units (PMUs) inform powerful diagnostic tools that can help avert catastrophic failures in the power grid. Because of this, PMU measurement errors are particularly problematic, and it is critical to understand their impact. However, there is limited understanding of how much the PMU measurement errors affect the performance of various synchrophasor-based applications, and thus the ability of these applications to fulfill the users' requirements effectively is also unclear. This paper examines internal and external factors contributing to PMU phase angle and frequency measurement errors. A generic method is proposed to evaluate the impact of measurement errors on application performance. The impact of measurement errors on several synchrophasor-based Wide Area Monitoring System (WAMS) applications are analyzed as examples. These applications include power system disturbance location, oscillation detection, islanding detection, and dynamic line rating. The analysis demonstrated that the proposed method can be used to quantify the measurement error impact and analyze the performance degradation of these applications due to the measurement error. It also reveals that the impact of measurement error depends on the type, algorithm, and parameters of applications.

INDEX TERMS Frequency, measurement errors, phasor measurement units (PMUs), power grids, synchrophasor, wide area measurements.

I. INTRODUCTION

Wide Area Monitoring System (WAMS) improves the situation awareness of power system by providing system states in fast and dynamic operation conditions, as well as unforeseen situations in a wide range [1]–[9]. Synchrophasors estimated by phasor measurement units (PMUs) are the major data used by WAMS applications. The performance and reliability of these end-use applications depends on data quality of synchrophasors [10]. Measurands, including phasor, frequency, and Rate Of Change Of Frequency (ROCOF), are subject to measurement errors from both internal and external factors, which may degrade the performance of applications or even cause them to fail.

Performance requirements of PMU measurements are specified in the IEEE/IEC Standard 60255-118-1:2018 [11]. The maximum allowed measurement error, such as total vector error (TVE), frequency error (FE), and rate of change of frequency error (RFE) have been defined. The effect of measurement error, however, depend on the specific application and its algorithm. E.g. locating a generations trip needs more accurate data than simply detect it. Therefore, the impact on the performance of the synchrophasor-based applications needs to be evaluated. Without understanding how the measurement errors will impact the performance of various synchrophasor-based applications, the users are not able to implement them for

The associate editor coordinating the review of this manuscript and approving it for publication was Md. Apel Mahmud.

This work is licensed under a Creative Commons Attribution 4.0 License. For more information, see http://creativecommons.org/licenses/by/4.0/

power system monitoring and operation confidently and effectively.

This paper focuses on quantifying the impact of measurement errors and gives the results such as how much error or failure are caused by a given measurement error; what is the worst case for a specific application with measurement error; to achieve a specific performance, how accuracy the measurement should be.

Furthermore, we considered the measurement error from not only the PMU device, but the instrumentation channels. Formed by instrument transformers, connecting control cables, and attenuators, the instrumentation channels are used to scale down the power system voltage and current to the levels proper for driving relays, fault recorders, and other monitoring devices such as PMUs [12]. Testing and evaluation indicate that instrument transformers could introduce phasor error [13].

Some studies are conducted to reveal the influence of synchrophasor error on different applications. The investigations mainly focus on applications of state estimation [14]–[16], voltage stability assessment [17], [18], and line fault and outage [19], [20]. However, these studies are all based on specific applications and algorithms. There is not a systematic method proposed for the error impact analysis. Quite a few synchrophasor-based applications, including those already being implemented, have not yet been evaluated. Furthermore, the errors in some of these studies are assumed either as fixed values or to follow Gaussian distribution. In reality, the mean value of synchrophasor error is not necessary 0. For example, the instrumentation channel error, which are unavoidable in reality and cannot be ignored in some applications, introduces a bias to synchrophasor errors. During power system dynamics and faults, or due to the imperfection of synchronized timing, the mean value of synchrophasor error could deviate from 0, and the error distribution may not follow Gaussian distribution [21], [22].

In this paper, a systematic method is proposed to evaluate and quantify the impact of errors on synchrophasor-based application. With this method, the impact of different error ranges can be analyzed, and the application developers could recommend the required accuracy of PMUs to be used. In response to users' concern on the reliability of the application, failure rates and the worst cases could be obtained from the analysis, so the users could determine how to best use the application in their system without nuisance alarms. The measurement errors from both PMU and instrumentation channels are taken into consideration. Four real applications are evaluated as the specific case studies to demonstrate how the proposed method is used to quantify the error impact. Most of them are being operated on wide-area monitoring systems (WAMSs). The applications are realized in C# and the testing programs are in MATLAB. This study also evaluated how the requirements of synchrophasor measurement accuracy vary depending on the specific application algorithm.

This work makes the following contributions.

(1) To the best of the authors' knowledge, we first create the generic method to access the impact of PMU measurement errors. This method is applicable to all PMU based applications with either quantitative or qualitative output.
(2) Based on this method, the impact of measurement errors on four real synchrophasor-based applications are analyzed for the first time, and the quantified impact are presented. It answers the questions such as in how much percentage the error impact is tolerable, what is the worst case, and how the error of output distributes.
(3) The relation of measurement error impact and other parameters are revealed. For a specific synchrophasor-based application, the error impact could change with different input and algorithm parameters. The proposed method is able to reveal this dependence, which is demonstrated in case studies.
(4) The instrumentation channel error has not been considered in the previous publications regarding measurement error impact. This work analyzed the main factors contributing to the instrumentation channel error and demonstrated that in what scenarios this error should be considered. It also demonstrated the importance of calibrating the instrumentation channel error by case study and quantified result.

The rest of this paper is structured as follows. In Section II the measurement errors from PMUs and instrumentation channels are discussed, and the assumption of measurement errors in this paper is given. The evaluation method for PMU error impact is proposed in Section III. Section IV - VII are the case studies on four typical synchrophasor applications, namely power system disturbance location, oscillation detection, islanding detection, and dynamic line rating. The impacts are discussed, and the mitigations are proposed in Section VIII. Section IX concludes the paper.

II. MEASUREMENT ERROR ANALYSIS

The factors that contribute to PMU measurement errors mainly consist of two components: internal and external. The former indicates the errors of the PMU device itself, and the latter mainly derives from the instrumentation channel.

A. PMU DEVICE ERRORS

PMU device errors are derived from various of factors, such as estimation algorithm, ADC, timing accuracy, injected noise and harmonics [23]. PMU accuracy compliance specified in the IEE/IEC standard is used as the benchmark in this study [11].

According to the standard, the TVE, FE, and RFE should be within 1%, 0.005 Hz, and 0.1 Hz/s for M class PMU when there is no harmonics and out-of-band interference. With dynamic signal inputs, such as modulation, frequency ramping, and phase step change, the requirements are relaxed. E.g., TVE for modulation input should be within 3%, and the maximum allowed FE for frequency ramping is 0.01 Hz.

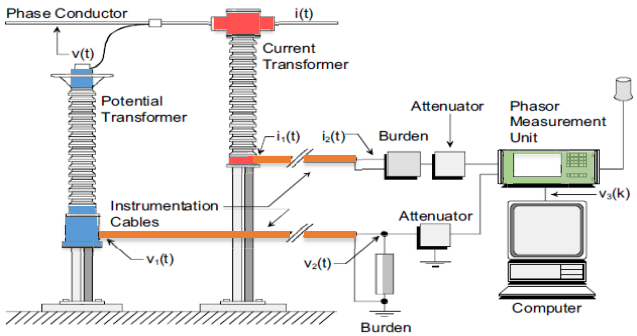

FIGURE 1. Typical instrumentation channel for a PMU.

B. INSTRUMENTATION CHANNEL ERRORS

The instrumentation channel in this paper refers to the circuit between the transmission system and the PMU. The instrumentation channel scales down the amplitudes of voltages and currents on the transmission system and passes them to the attached PMU. Components on the channel usually include instrument transformers, connecting control cables, burdens and attenuators, as shown in Fig. 1 [24].

An ideal instrumentation channel is supposed to output a waveform which is exactly a replica of the waveform scaled down from the high voltage power system [25]. The instrumentation channels in reality are not ideal and introduce measurement errors.

One contributor of instrumentation channel errors is the control cable, which introduces a time delay that is then transformed into phase angle error. This delay depends on several characteristics of the cable, such as the cable length, material, and whether it is shielded. Typically, a 500 ft. RG-8 cable introduces a 0.4° phase angle error. In some cases, the length of the cable can reach 3,000 ft., which will cause an even larger phase angle error [24].

Instrument transformer is another error source. The most commonly used instrument transformers include current transformers (CTs), voltage transformers (VTs), and capacitive coupled voltage transformers (CCVTs). For the American National Standards Institute (ANSI)–class type transformers, the maximum phase angle error allowed by the standard is between 0.26° and 2.08°, depending on the transformer type [26], [27].

While PMU devices are required to meet the requirements on TVE as discussed in II.A, there is no such requirement on a complete synchrophasor measurement system. Therefore, the performance of PMU-based applications could still be impacted even if the PMU devices are compliance with the corresponding standards. Furthermore, instrumentation channel error is usually not calculated and eliminated in some PMU installation procedures [28], [29]. This is partially because the actual value of the real system is constantly changing, and precise values are difficult to achieve. In this paper, the typical magnitude and phase angle error caused by instrumentation channels are assumed to be a constant value in the range from 0 to 0.52% and −1.55°, respectively, according to the testing cases in [26], [30]. The frequency error contributed by instrumentation channel is ignorable compared to the error from PMU device itself.

III. ANALYSIS METHODOLOGY

A. APPLICATION PERFORMANCE

The impact of PMU measurement errors is reflected in the performance of synchrophasor-based application. According to the output, the applications can be generally divided into two groups. One is with qualitative outputs, such as detecting and determining whether an islanding, oscillation, or fault is happening or happened. The other generates quantitative results, such as the event location, the amount of tripped generator, and the rating of a transmission line.

For the first group, bad outputs can be described as 'failure', including failed detection, e.g., failed to detect an islanding, or false alarm, such as triggering an alarm of oscillation while no oscillation happens. Here we define the failure rate r as

$$r = r_{FD} + r_{FA} = \frac{N_{FD}}{N} + \frac{N_{FA}}{N}, \tag{1}$$

where r_{FD} is the rate of failed detection, r_{FA} is the false alarm rate, N_{FD} is the number of event cases failed to be detected, N_{FA} is the number of non-event cases causing false alarms, and N is the total number of cases.

The failure rate due to the PMU measurement error, denoted as r_{err}, is used to quantify the error impact. It is defined as

$$r_{err} = r_{w/err} - r_{w/oerr}, \tag{2}$$

where $r_{w/err}$ is the failure rate when measurements with errors being injected into the application, and $r_{w/oerr}$ is the failure rate when the measurement is free of errors. Both $r_{w/err}$ and $r_{w/oerr}$ are calculated by (1).

For the second group, the impact is described by the error of the output results, i.e.

$$E_{err} = E_{w/err} - E_{w/oerr}. \tag{3}$$

In (3), E_{err} is the impact of measurement error, $E_{w/err}$ is the application output error when injected measurements are with error, and E_{noerr} is the application output error when there is no measurement error. Taking fault location as an example, $E_{w/err}$ is the distances from the calculated fault location to the real fault location using measurement data with measurement error; E_{noerr} represents the same distance but there is no measurement error in the input data.

B. IMPACT ANALYSIS

To calculate the quantified impact defined above, the application outputs with and without measurement error injected need to be obtained. For both groups, the outputs can be expressed as

$$y = f(x, p), \tag{4}$$

and

$$y + \Delta y = f\left(x + \Delta x, p\right), \quad \Delta x \in \left[e_{min}, e_{max}\right]. \tag{5}$$

In (4) and (5), x is the ideal PMU measurement (no error), Δx is the PMU measurement error, p represents other parameters used in this application, y is the output or failure rate with no error injection, and Δy is the change of output or failure rate when error is injected. x and Δx could be scalar or vector, depending on the number of PMUs used by the application. $[e_{min}, e_{max}]$ is the measurement error range assumed in the analysis.

To fully analysis the impact, the relation between Δy and Δx needs to be obtained, denoted as

$$\Delta y = f\left(x + \Delta x, p\right) - f\left(x, p\right) = s\left(x, \Delta x, p\right). \tag{6}$$

For the applications with qualitative output, the output $f(\cdot)$ denotes the failure rate or corresponding input, as defined in (1). To ensure the result is representative, a group of cases should be studied.

For the applications with quantitative output, if $f(\cdot)$ is a linear function for x, Δy will be independent of x, and (6) will become

$$\Delta y = f\left(\Delta x, p\right). \tag{7}$$

For most applications however, x and Δx cannot be decoupled. Therefore, the impact analysis needs to take different x, i.e. system status, into consideration. For some applications, the function $f(\cdot)$ is so complex that even for a fix x the analytical relation between Δy and Δx is hard to get. For the sake of this, Monte Carlo method can be used. A group of cases with different x should be used to obtain a generic conclusion. For each case, a cluster of Δx within the defined error range is generated and added to x. The results will be a cluster of r_{err} or E_{err}. Applying data analysis, the maximum, mean, and distribution of the impact can be obtained, and indicates the performance under PMU error impact.

Sometimes the global maximum impact of an application is desired to understand the worst case of an application. Based on (6), the maximum impact of one specific case can be represented by

$$\Delta y_i^{max} = \max_{\Delta x} s(x_i, \Delta x, p). \tag{8}$$

Here x_i represents the measurement input of case i, and Δy_i^{max} is the maximum error impact of this case. Then the global maximum impact can be calculated by

$$\Delta y^{max} = \max_i \Delta y_i^{max}, \tag{9}$$

where Δy^{max} is the global maximum impact of the application. For most cases, it is hard to obtain the analytical maximum value of function $s(\cdot)$ regarding Δx. Monte Carlo method then can be used.

Furthermore, by changing the range and/or distribution of the measurement error, the impact of application performance may subject to change. Hence, the dependence of performance impact on measurement error could be obtained.

In addition, Δy may also dependent on parameters p of the application function $f(\cdot)$. The results of Monte Carlo simulation can be used to analysis the sensitivity of these parameters.

C. ERROR INJECTION

In the impact analysis, one of the important steps is to inject PMU measurement error, i.e. Δx. To simulate the real applications, the injected error should be determined by analyzing the specific application algorithm.

The instrumentation channel error may be eliminated in specific applications. As the instrumentation channel error is typically a constant value for a specific set of devices, applications using measurement differences are immune to this error. E.g., angle of synchrophasor rotates within 0 to 2π when system frequency deviates from nominal frequency. Therefore, phase angles used in most applications are the relative value, i.e. the angle different between the object synchrophasor and the synchrophasor at the reference point, usually the swing bus. When the instrumentation devices and control cable lengths at both locations are very similar, their instrumentation channel errors are also close to each other and will be eliminated when calculating the phase angle. Similarly, when an application uses the difference between measurements at two different times but from the same measurement device, the instrumentation channel error is also eliminated.

The range of injected error may change depending on the power system status. For applications used during system normal status, PMU error of steady state should be used for assumption. For those applications used for system disturbance detection and analysis, the corresponding dynamic error should be considered. E.g., oscillation detection should use the PMU error with modulated signal input; generation trip should use the error when PMU is fed with frequency ramp signal.

IV. POWER SYSTEM DISTURBANCE LOCATION

A. SYNCHROPHASOR-BASED DISTURBANCE LOCATION ALGORITHM

Power system disturbance location is a PMU application used to detect and locate power grid disturbance events, such as generator loss and load shedding. This case study analyzed the power system disturbance location application used by the Frequency Monitoring Network (FNET) in service at the University of Tennessee, Knoxville and some electric utility operation centers [31], [32].

When generator loss or load shedding happens, the active power of the system experiences a sudden change. According to the swing equation [33], there is

$$\frac{2H}{\omega_s} \cdot \frac{d^2\delta}{dt^2} = \Delta P, \tag{10}$$

where H is the inertia, ω_s is the system angular frequency, δ is the rotor angle, and ΔP is the difference between mechanical power injection and the electrical power withdrawn by

the load. $d^2\delta/dt^2$ is the acceleration of the rotor angle. Under normal operation conditions, the mechanical power injection and the load consumption are balanced, the rotation speed of the synchronous machine keeps constant, and $d^2\delta/dt^2$ is zero. During a power system disturbance, the rotor decelerates or accelerates with respect to the mismatch of power generation and consumption, i.e. ΔP. As the frequency f is the time derivative of angle, i.e.

$$f = \frac{1}{2\pi} \cdot \frac{d\delta}{dt}, \tag{11}$$

(10) can be rewritten as

$$\frac{2H}{\omega_s} \cdot \frac{2\pi df}{dt} = \Delta P. \tag{12}$$

For an interconnection, in which many generators and loads are included, an aggregated model of the system can be constructed based on the superimposing of the synchronous machines and loads, i.e.

$$\frac{2H_{sys}}{\omega_s} \cdot \frac{2\pi d\hat{f}}{dt} = \Delta P_{sys}, \tag{13}$$

where H_{sys} is the system inertia aggregated by all generators' inertia; $\hat{f}$ is the average frequency observed in the network, and ΔP_{sys} is the difference between aggregated power injection and the aggregated electrical power load [34]. With (13), the power system dynamics during disturbance can be analyzed.

ROCOF is defined as the time derivative of frequency and can be represented by

$$ROCOF = \frac{df}{dt} = \frac{1}{2\pi} \cdot \frac{d^2\delta}{dt^2}. \tag{14}$$

By combining (13) and (14), we obtain

$$ROCOF = \frac{\Delta P_{sys} \cdot f_s}{2H_{sys}}. \tag{15}$$

Here f_s is the system frequency. During the steady state, ROCOF is 0. For a single generator loss or load shedding event, ROCOF is a non-zero constant value.

Denote the angle of the synchrophasor measured by an FDR as θ. With the first and second derivative of phase angle described in (11) and (14) respectively, θ can be represented by

$$\theta = \pi \cdot ROCOF \cdot t^2 + 2\pi f_s \cdot t + \theta_0 \tag{16}$$

where θ_0 is the phase angle at time 0. The phase angle after disturbance follows the quadratic function of time. This change of phase angle does not simultaneously take place on all the buses in the power system. Instead, it propagates along the power network with finite and constant speeds [35]. This is also known as the electromechanical wave. Because of this, the variation of phase angle detected by each PMU has a unique time delay proportional to the distance from the disturbance location. The location of the disturbance can be estimated based on this relationship. When implemented in FNET, frequency disturbance recorders (FDRs), a type of single-phase distribution-level PMUs, are used to collect GPS timestamped voltage phasors and frequency measurements.

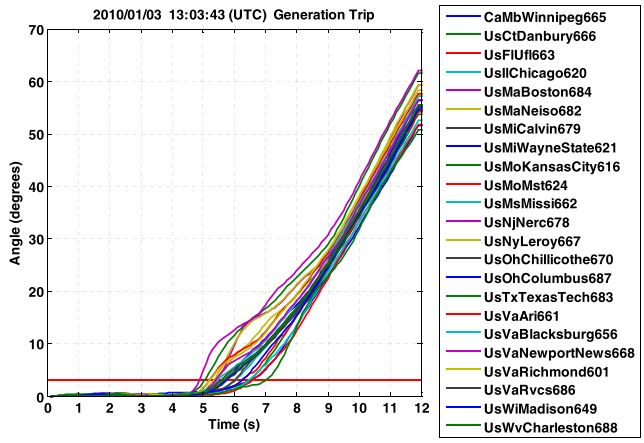

FIGURE 2. The plots of processed phase angle measured by FDRs in a generation trip event. The red horizontal line represents the preset threshold which is used to calculate TDOA.

In the application, the angles are shifted to start from 0° and the slope of the plot before the disturbance is de-trended to be 0 [32]. In this way, only the dynamic signature of different FDRs in reaction to the power system disturbance is reserved. The absolute values of these angles are then taken for the disturbance location. Fig. 2 shows an example of phase angle movements caused by a generation trip.

Coordinated Universal Time (UTC) is used to indicate the time at which the disturbance occurred. The legends show the names of the different FDRs used by FNET. The red horizontal line in Fig. 2 represents the preset threshold, denoted as θ_{TH}. The earliest time when the angle measured by an FDR increases to this threshold is defined as time difference of arrival (TDOA). It can be seen from Fig. 2 that the TDOAs of FDRs are different.

The first few responding FDRs are used for disturbance location. Their geographic coordinators and TDOAs are presented in (17).

$$(x_i - x_0)^2 + (y_i - y_0)^2 = V(t_i - t_0). \tag{17}$$

In (17), x_i, y_i and t_i are the longitude, latitude, and TDOA of the FDR with index i, respectively; x_0, y_0 and t_0 are the longitude, latitude, and TDOA at the disturbance location, respectively; V is the propagation speed. Disturbance location (x_0, y_0) can be estimated by least square method. Most disturbances detected are generation trips.

B. PMU MEASUREMENT ERROR IMPACT ANALYSIS

In the power disturbance location algorithm introduced in last subsection, the constant and linear part of θ in (16) are eliminated during angle processing. The processed angle is represented by

$$\theta = \pi \cdot |ROCOF| \cdot t^2. \tag{18}$$

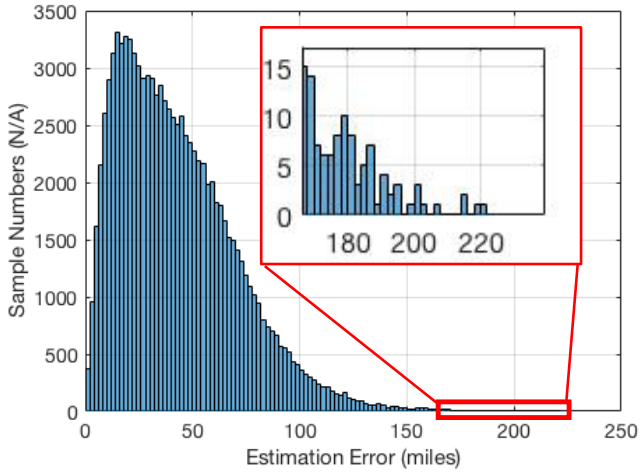

FIGURE 3. Location estimation errors distribution of one case.

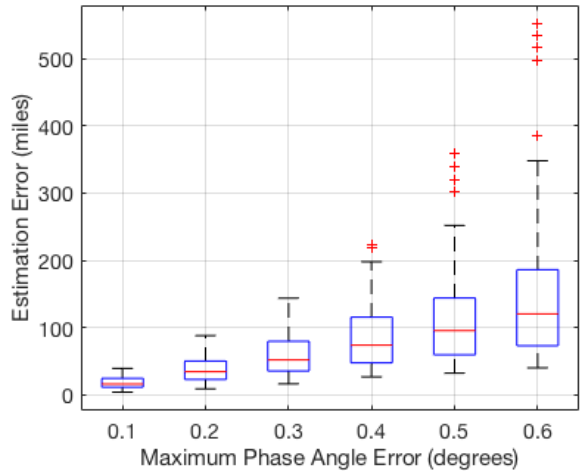

FIGURE 4. Boxplots of location estimation errors distribution regarding different maximum phase angle errors.

The angle error, denoted as θ_{err}, furtherly becomes TDOA error, denoted as t_{err} and represented by

$$t_{err} = \frac{\theta_{err}}{\frac{d\theta}{dt}\big|_{\theta=\theta_{TH}}} = \frac{\theta_{err}}{2\sqrt{\pi\theta_{TH}\,|ROCOF|}}. \tag{19}$$

This application generates a quantitative result, i.e. the location of the power system disturbance. Therefore, it belongs to the second group stated in III.A. The error of the disturbance location incurred by θ_{err} can be obtained based on (6).

As the relation between (x_0, y_0) and t_i is nonlinear, and TDOAs from multiple units are used for estimation, it is difficult to directly obtain the impact of PMU measurement error. Monte Carlo simulation is implemented here. A group of real power system disturbance cases in the Eastern Interconnection (EI) of the North America Power Grid are studied. For each case, different θ_{err} are tested and the results are compared. Here θ_{err} is randomly distributed in the range of $[-0.6°, +0.6°]$. The range corresponds to the largest phase angle error in a frequency ramping event allowed by PMU standard, i.e. 1% TVE [11].The result of one case is shown in Fig. 3.

The estimation errors of over 96% samples are within 100 miles; however, the error surpasses 180 miles in some cases. The largest possible error reaches 220 miles. It should be notified that for a large transmission grid as EI, in general the change of power needs to be as large as 300 MW to induce enough change of frequency and phase angle and trigger the disturbance location application. Power stations of that size are typically far from each other. With a 100-mile error it is still able to locate the tripped plant, by looking up the table of power plant locations and capacities. Empirically, an estimation error larger than 225 miles could cause failure in EI system [32].

To best use this application, it is desired to understand the worst case, which indicates the maximum possible error of the event location. To obtain the largest event location error, the Monte Carlo simulation is first implemented. Then the interior-point algorithm is used, with the θ_{err} of each unit corresponding to the largest fault location in the Monte Carlo simulation as the initial value. All detected cases in one year are analyzed, and the distributions of maximum event location estimation errors are plotted regarding different maximum θ_{err}, as shown in Fig. 4.

According to the result, the medium and maximum values of location estimation error increase with the maximum phase angle error. The maximum estimation error is roughly proportional to the maximum phase angle error; it increases from 50 miles to over 300 miles when the maximum phase error changes from 0.1° to 0.6°. The deviation of the estimation error also increases with the maximum phase angle error. When the estimation error is small, it is easier to improve the location accuracy by estimate the amount of power change and inspect possible generators around the estimated location. If the estimation error is too large, this application will give incorrect result or fail. When the phase angle error increases to 0.4°, the cases with estimation error over 225 miles emerges, and with 0.6° error, around 20% cases could get an error over 225 miles, resulting the application failure. It should be noticed that these results only indicate the worst possible results and does not mean these percentage of cases will surely fail.

According to (19), TDOA error is inversely proportional to the square root of $|ROCOF|$. When θ_{err} remains unchanged, the error will decrease with the increase of $|ROCOF|$. However, θ_{err} usually depends on $|ROCOF|$ in a frequency ramping event. Taking the PMU algorithm in the appendix of [11] as an example, the maximum θ_{err} is proportional to $|ROCOF|$. In that case, a larger generation trip will induce a larger $|ROCOF|$ according to (15), and hence larger estimation location error.

With the increasing penetration of inverter-based renewables, the inertial of the power system will expect to decrease. As a result, $|ROCOF|$ will increase according to (15). This change calls for higher PMU accuracy in the future.

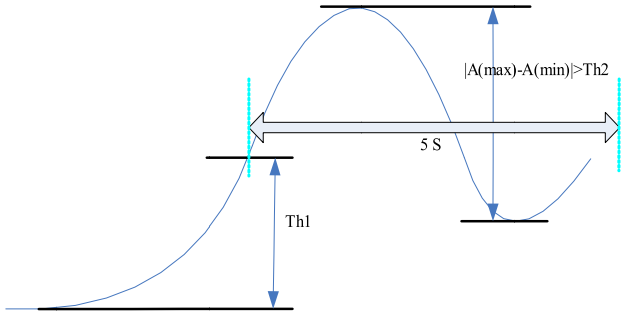

FIGURE 5. Schematic of angle-based oscillation detection.

V. OSCILLATION DETECTION

A. OSCILLATION DETECTION ALGORITHM

Small signal stability problems in a power system can result in significant electromechanical oscillations that may lead to grid stability issues and potentially large-scale black-outs. High-precision and time-synchronized frequency and phase angles measured by PMUs can be used for oscillation detection.

Here the angle-based inter-area oscillation detection is used as an example [1]. In this application, relative angle measurements of each PMU are obtained by subtracting a reference PMU's measurement and shifting to start from 0°. These angle measurements remain stable when the system is operating in the steady state. During an inter-area oscillation, the relative angles form a wavy curve. The signature of an oscillation event usually shows a data pattern that has a steep angle rise or drop beyond a certain threshold right after disturbance and then, following the oscillation starting point, the oscillation magnitude (peak-to-peak value) goes beyond a certain limit and the oscillation is sustained for at least one swing. The schematic diagram for this is shown in Fig. 5.

If the oscillation deviation of more than one PMU surpasses the preset Threshold 1 (denoted as Th1) and the oscillation magnitude exceeds the preset Threshold 2 (denoted as Th2) and sustains for at least one swing within 5 seconds, an oscillation will be considered to occur. Th2 is the key value to determine whether a swing is an oscillation. The thresholds are empirical values and are determined by the power grid under observation. Taking EI as an example, Th1 and Th2 are set as 4° and 3°, respectively.

B. PMU MEASUREMENT ERROR IMPACT ANALYSIS

Similar to the disturbance location, instrumentation channel errors are ignored as they are constant values and are eliminated when the relative angle is calculated and shifted to start from 0°. For an oscillation event, the oscillation magnitude with error could be smaller than the thresholds, and the oscillation would not be detected. On the other hand, a false alarm would be triggered if the variation magnitude of a non-oscillation signal is affected by the measurement error and surpasses the thresholds.

A real oscillation case in the EI is shown in Fig. 6, with a 1.2° error band represented by green shadow.

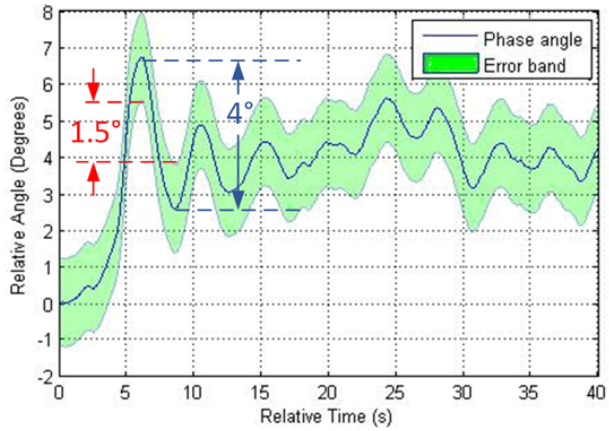

FIGURE 6. Phasor measurement unit error impact on oscillation signal.

The oscillation magnitude is about 4°, larger than Th2 (3°) and should be detected if there is no error. However, accounting for the measurement error, the angle difference could decrease to 1.5°, which is below Th2 – the oscillation would not be detected.

As oscillation detection is a qualitative application as described in III.A, the impact can be quantified by failure rate difference defined by (2). As the oscillation detection algorithm studied here is a non-linear function, (6) is used to calculate the impact, i.e. the failure rate induced by the error. The failure includes both failed detection and false alarm, and the failure rate of each is obtained separately. In all studied oscillation cases, the failure rate are 0 when inputting clean data. Therefore, (6) can be simplified to

$$\Delta y = f_{osc}\left(x + \Delta x, p\right), \tag{20}$$

where x represents the clean data of phase angles, Δx is the phase angle error, f_{osc} is the oscillation detection algorithm, Δy is the output, denoting the failure rate, and p represents the parameters, such as the angle fluctuation of the input signal.

In the PMU standard [11], TVE is required to be within 3% for modulated signal input, corresponding to 1.8° for 60 Hz system. Different error levels are tested in this study. Monte Carlo simulation indicates that for a confirmed oscillation event, the angle error is unlikely to cause failed detection, and the failure rate is nearly 0. However, for a non-oscillation fluctuation, phase angle errors could induce false alarm, depending on the angle fluctuation of the input signal. The simulation result is shown in Fig. 7.

Results indicates that the false alarm rate increases with the phase angle error. Meanwhile, the signal with higher fluctuation amplitudes in angle is more vulnerable to phase angle error. E.g., if the fluctuation amplitude is 0.8°, the phase angle error below 1.3° will not cause false alarm; for the fluctuation amplitude of 1.6°, however, 0.6° error could cause false alarm. If the fluctuation amplitude is as large as 2.4°, PMU error as small as 0.1° could cause false alarm, and 0.4° phase angle error could cause 100% false alarm.

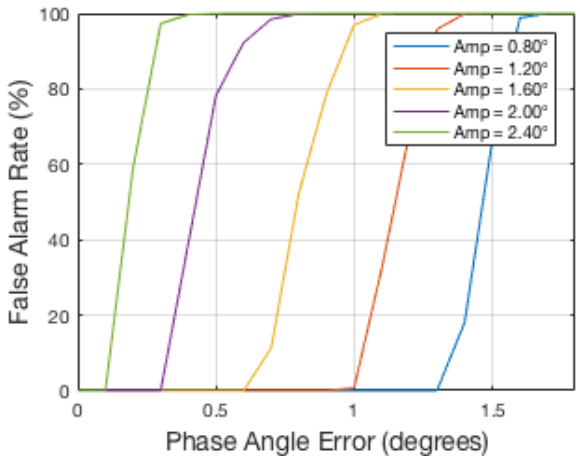

FIGURE 7. False alarm rate of angle-based oscillation detection regarding different phase angle errors and fluctuation amplitudes.

Although phase angle error has little impact on misdetection of oscillation, false alarm could also degrade the performance and trustworthy of the application. Therefore, the requirements of synchrophasor accuracy needs be specified and can be determined according to the fluctuation at the monitoring point of the power grid.

VI. ISLANDING DETECTION

A. ISLANDING DETECTION ALGORITHM

Distributed generation (DG) sources, which use fuel cells, photovoltaic, and other electricity generation technologies, are typically placed close to the load being served [36]. The advantages of DG are well known. However, there are some technical challenges associated with the use of DG. One of them is islanding, the situation when part of a distribution system becomes electrically isolated from the remainder of the power system while continuing to be powered by DG sources. Electrical islands are difficult to sustain and typically result in loss of service to the loads. They can also threaten the safety of line workers if the workers are not aware that the circuit is energized. Reconnecting the island to the larger system requires that both are in synchronicity, but the DG sources often cause them to drift out of phase. Therefore, it is very important to detect islands quickly in order to reconnect them before the generation and load become unbalanced and the load is lost.

PMUs capture the characteristics of frequency and phase angle change during the creation of the island in a fast and accurate manner. Using PMUs in islanding detection is therefore promising. Here we take the frequency measurement based islanding detection method running on FNET as an example [37]. In this algorithm, frequency deviations (FD) of each FDR is calculated by

$$FD_i\,(t) = |f_i\,(t) - f_{\mathrm{ref}}(t)|\,, \tag{21}$$

where $f_i(t)$ is the measured frequency value of the i-th FDR at timestamp t; $f_{\mathrm{ref}}(t)$ is the median value of all the monitored FDRs in the same interconnection. The integration of frequency deviation (IOFD) is defined as the accumulation of the corresponding FD over a certain period of time, given by

$$IOFD_i = \sum\nolimits_{t_1}^{t_2} FD_i(t), \tag{22}$$

where t_1 and t_2 are the start time and end time, respectively, for this integration time period. IOFD is used to prevent the algorithm from causing a false alarm. For example, an abnormal frequency data point far away from the actual value will generate a large FD. Also, during a generation trip event, the grid remains intact yet the frequency in some locations may oscillate while dropping. If FD is the only criterion, this kind of phenomenon could be incorrectly recognized as an islanded situation.

When the FD_i of any FDR surpasses the first threshold, Fth_1, an early warning is triggered, indicating possible islanding. Then $IOFD_i$ is calculated and compared to the second threshold, Fth_2. If it is larger than Fth_2., the algorithm concludes that the system monitored by this FDR is in off-grid operation. Otherwise, the system is deemed as not islanded.

B. PMU MEASUREMENT ERROR IMPACT ANALYSIS

When measurement error is combined with the frequency, the result of FD_i and $IOFD_i$ will be influenced, causing the islanding detection algorithm to fail to detect an island or to incorrectly indicate an islanded situation when no island exists. To demonstrate islanding detection errors, cases are selected, and data collected by FDRs are fed into the algorithm to verify that the algorithm is functioning correctly. Frequency errors are then added to the data and the new detection result is compared with the original one to identify the impact caused by the measurement error.

Similar to oscillation detection, islanding detection is also a qualitative application, and the PMU error impact is defined by (2). Similarly, (6) is used to calculate the failure of each case. Because the islanding detection algorithm is non-linear, and the failure rates of all cases studies are 0 when no error is injected, (6) is furtherly simplified to the following equation.

$$\Delta y = f_{isld}\,(\boldsymbol{x} + \Delta\boldsymbol{x}, \boldsymbol{p}) \tag{23}$$

In (23), vector $\boldsymbol{x}$ represents the clean data of frequency at different measurement locations, $\Delta\boldsymbol{x}$ is the vector of frequency errors of each location, f_{isld} is the islanding detection algorithm, Δy is the output, i.e. failure rate, and $\boldsymbol{p}$ represents the parameters such as the detection time $t_2 - t_1$ and the average frequency deviation in the islanding area.

One case study occurred during Hurricane Sandy in 2012. During that time, the off-gird operation was detected by an FDR in Sussex, New Jersey. The frequencies are plotted in Fig. 8.

In the experiment, errors within ±5 mHz are added to the data. However, due to the large frequency deviation, the added errors are not large enough to be the cause that the islanding detection algorithm failed. Further analysis shows that the islanding detection would not fail until the frequency error is larger than ±0.35 Hz.

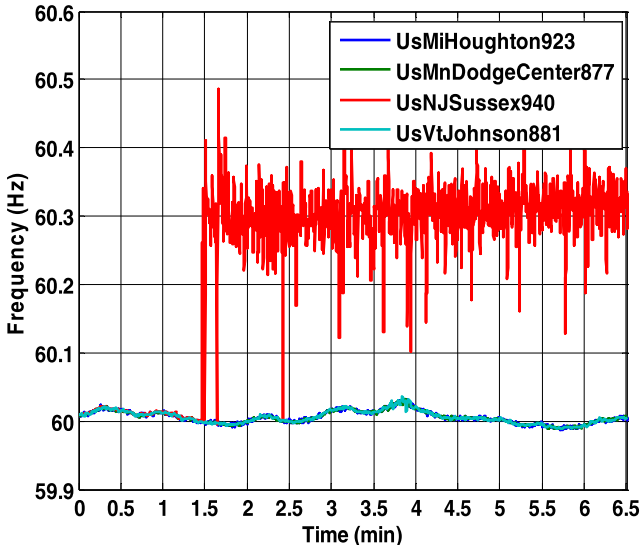

FIGURE 8. Frequency measured by frequency disturbance recorders during Hurricane Sandy case shows the Sussex FDR (in red) operating in an island.

Several other cases are also studied by adding frequency errors and changing the integration time. The islanding detection time of this algorithm mainly depends on the integration time of IOFD. Analysis shows that the ±5 mHz error does not influence the detection accuracy on detection time from 2 s to 30 s. No islanding event is missed by the algorithm, nor does any false alarms take place. The corresponding failure rates are 0.

The success rate of detecting an island depends on the thresholds selection and the generation-load imbalance of the island. For an island in which the imbalance is very small, this method will be vulnerable to frequency errors.

VII. DYNAMIC LINE RATING

A. DYNAMIC LINE RATING ALGORITHM

The rating of a transmission line indicates the highest current that the line can transfer safely and securely. Currently, the ampacity of the transmission lines are generally determined by conservative seasonal estimations of meteorological values [38]. Dynamic line rating (DLR) technology is developed to calculate this ampacity at each time unit of operation. The application of DLR can dynamically increase the transmission capacity and effectively use the thermal capacity of the transmission line (assuming there are no stability limits), especially for the overhead transmission lines. As intermittent renewable energy sources put stress on the existing infrastructure of the power system, DLR provides a solution to accommodate the surge in installation of distributed/renewable energy sources while minimizing or postponing the high cost of power network enforcement [38].

PMU measurement data can be used to dynamically calculate the rating of that line. One method based on IEEE Standard 738-2012 is used here as an example [39]–[41]. In this method, the phasors of voltage and current measured by PMUs installed on both ends of a transmission line are used to obtain the line resistance. Together with the weather data measurement, the dynamic line rating is calculated. The procedure is shown in Fig. 9.

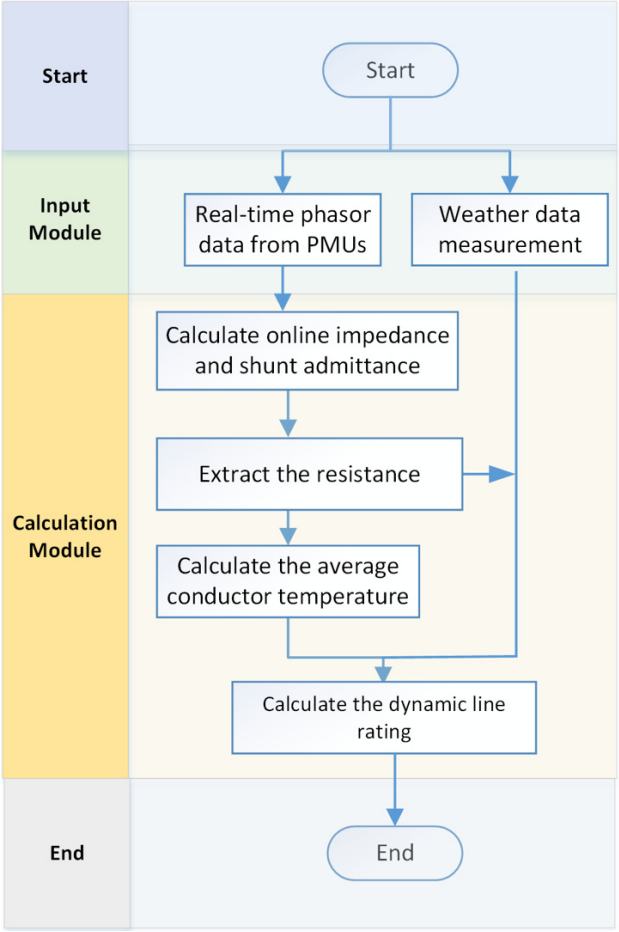

FIGURE 9. Overall framework of phasor measurement unit (PMU)–based dynamic line rating technology.

B. PMU MEASUREMENT ERROR IMPACT ANALYSIS

The PMU measurement error could induce uncertainty in the estimation of the transmission line parameter. As the output of dynamic line rating application is quantitative, the error impact is calculated based on (3). Because magnitude measurement can be corrected by voltage and current sensors with high accuracy, here we only consider the phase angle error, which includes ±0.6° error from the PMU and 0° to −1.55° error from the instrumentation channel, as assumed in II.B. In this studied case, the conductor of the transmission line is the 26/7 Drake aluminum conductor, steel-reinforced (ACSR) conductor. The configuration and the parameters of the conductor are based on [41]. The DLR model in this system is assumed to refresh every 10 min. In this application, the relation between line rating and phase angles is non-linear, so (6) is used to get the impact of PMU measurement error. Monte Carlo simulation is implemented by adding multiple combinations of errors to the voltage and phase angles on both terminals of the transmission line. Each phase angle error is

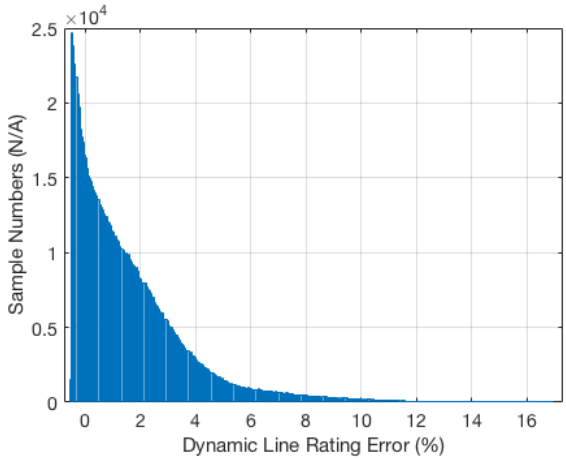

FIGURE 10. Distribution of dynamic line rating error of one case.

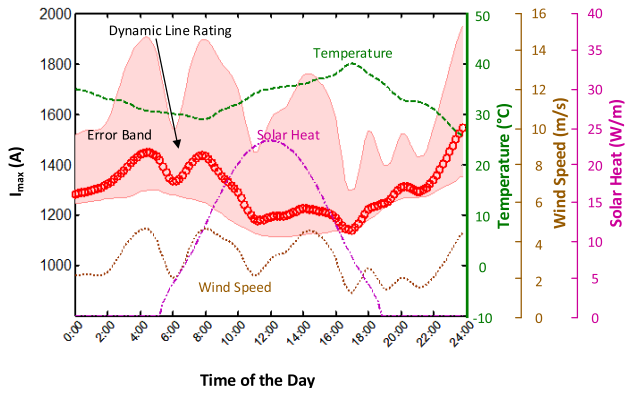

FIGURE 11. Dynamic line rating error on one day in summer.

the addition of both PMU device error and instrumentation channel error.

The effect of PMU measurement error depends on the weather condition. In this case study, weather parameters are assumed to be consistent, with ambient temperature, wind speed, and solar heat gain being 30°C, 1 m/s, and 12 W/m, respectively. Totally 10^6 error combinations are randomly picked and simulated in the study, and the histogram of DLR error is shown in Fig. 10.

According to the simulation result, the DLR error caused by the measurement error ranges from −5% to 16.93%. In 93.17% samples the DLR errors are less than 5%, and 99.74% of them are within 10%.

To understand the worst result under the impact of the PMU measurement error, the maximum DLR error is evaluated under various weather conditions. The result of one-day in summer is shown in Fig. 11.

In this figure, the red-circle line represents the true value of DLR, and the red shadow represents the error band. The green, brown, and purple dashed curves are the ambient temperature, wind speed, and solar heat gain, respectively. According to the calculation, the maximum error in summer with high wind speed reaches 46%. For a case with lower temperature and wind speed, the maximum error decreases to

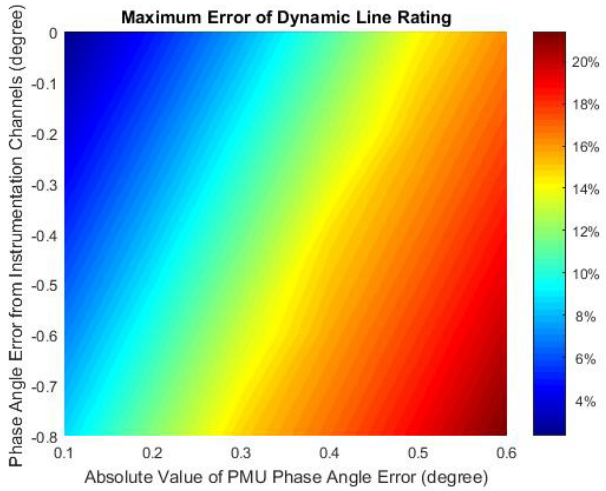

FIGURE 12. Maximum DLR error respect to PMU phase angle error and instrumentation channel phase angle error in a low temperature and wind speed day. The error is in percentage. PMU phase angle error is positive and negative boundary.

approximately 22%. It should be noted that these only indicate the worst cases under very high and low temperatures. For most cases, the DLR error is much smaller than these extreme values. Also notice that these examples are obtained from a basic method and are not intended to give a specific DLR error boundary.

The relation between maximum DLR error and measurement error for a low temperature and wind speed day is shown in Fig. 12.

From this figure, it can be seen that the maximum error will decrease from 22% to 16% if the instrumentation channel error is eliminated (e.g., by calibration). With −0.8° phase angle error contributed from instrumentation channel the PMU error should be as accurate as ±0.1° to ensure the maximum DLR error is below 10%. By calibrating the instrumentation channel error, the requirement of PMU accuracy could be relaxed to ±0.3°, i.e. only one third accuracy requirement of the PMU without this calibration. This is an effective way to improve the accuracy of the dynamic line rating.

VIII. DISCUSSION

A. SYNTHESIS OF RESULTS

The result obtained in this study can be synthesized as follows.

1) POWER SYSTEM DISTURBANCE LOCATION

measurement error can result in location estimation failure. With the PMU error of ±0.6°, typically over 90% location errors induced by inaccurate measurement is within 100 miles and tolerable. However, when considering the worst cases, more than 50% of them are possible to generate an estimation error over 100 miles. With the increasing of DERs and the decreasing of system inertial, smaller phase angle error will be required to achieve the same location estimation accuracy.

2) POWER SYSTEM OSCILLATION DETECTION

measurement error is unlikely to result in failing to detect but could cause false alarm. The probability of false alarm depends on the selection of detection threshold, fluctuation amplitude of the observed signal, and the phase angle error. In EI, if the fluctuation amplitude is up to 2.4°, a 0.1° measurement error is enough to generate a false alarm, and 0.4° phase angle error could cause 100% false alarm.

3) ISLANDING DETECTION

measurement error is unlikely to influence the frequency-based islanding detection when the generation and load imbalance is large. If generation and load are close to each other and the detection time window is short, the frequency deviation may be submerged in the frequency measurement error and the application may failed to detect an islanding.

4) DYNAMIC LINE RATING

the error of this application shows dependency to the parameters related to weather conditions. Under the normal weather condition, the thermal rating error is within 5% in 90% cases, with the maximum error of 16% (worst case). In severe weather conditions, the maximum error can reach up to 46%. Meanwhile, the phase angle error introduced by the instrumentation channel contributes considerably to the total error.

B. PMU ERROR

In this paper, the PMU phasor and frequency errors are assumed based on the requirement of IEC/IEEE 60255-118-1:2018 standard. They are random values within 1% TVE and ±0.005 Hz, respectively during steady state. For dynamic inputs such as phase and magnitude modulation, the permitted error range is even larger, e.g. 3% TVE for phasor error. According to the analysis presented in this paper, a standard compliance PMU does not guarantee the performance of all applications. Same amount of PMU error has different performance impact depending on the type, algorithm, parameters, and other inputs of the application.

In the four applications studied in this paper, most cases are not influenced when the PMU is compliance with the standard. In abnormal conditions the error impact may increase. For example, phase angles with large fluctuations may lead to higher possibility of false alarm in oscillation detection. An islanding area with small generation-load imbalance may not be detected by the islanding detection application. Developers and users could use the method proposed in this paper to evaluate the impacted performance and determine if the PMUs with higher accuracy are required, or the algorithm should be improved.

Furthermore, the maximum error impact studied in this paper indicates the worst cases that could happen. In the applications we studied here, these cases are either rare, or only happen at extreme and/or abnormal conditions. Mostly, they can be ignored. However, for applications used for power system control, these worst cases may cause large impact to the system, hence should be fully evaluated and addressed.

C. INSTRUMENTATION CHANNEL ERROR

Instrumentation channel error, if not calibrated, would introduce an offset in phase angle measurement. Unlike voltage and current magnitude, usually there is no other devices in substations to provide a reference for phase angle, so instrumentation channel error may remain in the measurement. Some applications use relative changes of phase angles, such as disturbance location and oscillation detection discussed in this paper. This constant error is therefore eliminated and is unlikely to influence the corresponding applications. However, in some other applications, such as dynamic line rating, the measurements are directly used, and instrumentation channel error could cause large impact.

No particular standards have been published for phase angle error calibration of the instrumentation channel to which PMUs are connected. Two software-based methods can be considered for instrumentation channel calibration. One is to model the instrumentation channel and calculate the error; the other is using state estimation methods to correct the instrumentation channel error [30], [42]. Some PMUs provide user configurable settings for phase and magnitude correction factors. How to precisely calibrate the instrumentation channel error is out of the scope of this paper. Further work is needed to develop methods to characterize and correct the instrumentation channel errors.

D. RECOMMENDATIONS

PMU measurement errors could impact the performance of synchrophasor-based applications. Without the awareness of the existence and the effect of the impact, the application users may be misled by the influenced outputs and make wrong decisions, and the applications cannot be implemented confidently and effectively. As the measurement error cannot be fully eliminated, it is recommended for the PMU application developers and users to:

- Evaluate the performance of the applications by considering the actual measurement error. The method proposed in this paper can be used to quantify the error impact.
- For applications with high requirement on every output, such as those for power system control, the worst cases and their impact should be evaluated.
- Analyze whether the instrumentation channel would contribute to the measurement error. If so, the developer and/or user should analyze its impact and decide if calibration is required.

Approaches to decrease or eliminate the measurement error impact include upgrading PMU hardware and algorithm, calibrating PMU and instrumentation channel, and improving application's error tolerance [30]. These approaches relate to the specific devices and algorithms being used and will be included in the continuous study.

IX. CONCLUSION

In this paper, a generic method is proposed to analyze and quantify the impact of error on synchrophasor-based applications. Depending on the output of the object application, the method evaluates its failure rate or error distribution under the impact of the given synchrophasor accuracy range. It can be used to determine the desired accuracy level of synchrophasor measurement. This method could also be used for sensitivity analysis on parameters of application algorithm or the input signal, based on which the application can be optimized.

The impact of PMU measurement errors on four typical applications is studied. The measurement errors from both the PMU device itself and the instrumentation channel are investigated. According to the analysis, measurement errors could result in applications mal-operation, including incorrect disturbance location, false alarm of oscillation, and error of transmission line thermal rating. Though all these applications have different measurement error tolerance, most of them are potential to be influenced.

The analysis method demonstrated in this paper can aid other developer and user in identifying and quantifying the measurement error impact, the pervasiveness in deployed systems, the desired PMU and instrumentation channel accuracy. With a full evaluation of the impact from all possible measurement error, the synchrophasor based applications can be used for power system monitoring and operation with knowledge of its performance. In addition, the assessment from the evaluation can lead to the development of new technologies resilient to measurement error.

REFERENCES

[1] T. Xia, Y. Zhang, L. Chen, Z. Yuan, P. N. Markham, Y. Ye, and Y. Liu, "Phase angle-based power system inter-area oscillation detection and modal analysis," *Eur. Trans. Electr. Power*, vol. 21, pp. 1629–1639, Nov. 2011.

[2] Z. Lin, T. Xia, Y. Ye, Y. Zhang, L. Chen, Y. Liu, K. Tomsovic, T. Bilke, and F. Wen, "Application of wide area measurement systems to islanding detection of bulk power systems," *IEEE Trans. Power Syst.*, vol. 28, no. 2, pp. 2006–2015, May 2013.

[3] R. Mai, L. Fu, and H. Xu, "Dynamic line rating estimator with synchronized phasor measurement," in *Proc. Int. Conf. Adv. Power Syst. Autom. Protection (APAP)*, Beijing, China, Oct. 2011, pp. 940–945.

[4] W. Yao, J. Zhao, M. J. Till, S. You, Y. Liu, Y. Cui, and Y. Liu, "Source location identification of distribution-level electric network frequency signals at multiple geographic scales," *IEEE Access*, vol. 5, pp. 11166–11175, 2017.

[5] Y. Liu, W. Yao, D. Zhou, L. Wu, S. You, H. Liu, L. Zhan, J. Zhao, H. Lu, W. Gao, and Y. Liu, "Recent developments of FNET/GridEye—A situational awareness tool for smart grid," *CSEE J. Power Energy Syst.*, vol. 2, no. 3, pp. 19–27, 2016.

[6] S. You, Y. Liu, T. Micah, J. Zhao, W. Yao, D. Zhou, L. Wu, Y. Su, X. Zhang, and Y. Liu, "Disturbance location determination based on electromechanical wave propagation in FNET/GridEye: A distribution-level wide-area measurement system," *IET Gener., Transmiss. Distrib.*, vol. 11, no. 18, pp. 4436–4443, 2017.

[7] A. Sharafi, M. Sanaye-Pasand, and F. Aminifar, "Transmission system wide-area back-up protection using current phasor measurements," *Int. J. Elect. Power Energy Syst.*, vol. 92, pp. 93–103, Nov. 2017.

[8] J. Lin, Y. Su, Y. Cheng, C. Lu, L. Zhu, H. Huang, and Y. Liu, "A robust complex-domain state estimator using synchrophasor measurements," *Int. J. Elect. Power Energy Syst.*, vol. 96, pp. 412–421, Mar. 2018.

[9] M. Li, A. Pal, A. G. Phadke, and J. S. Thorp, "Transient stability prediction based on apparent impedance trajectory recorded by PMUs," *Int. J. Elect. Power Energy Syst.*, vol. 54, pp. 498–504, Jan. 2014.

[10] J. De La Ree, V. Centeno, J. S. Thorp, and A. G. Phadke, "Synchronized phasor measurement applications in power systems," *IEEE Trans. Smart Grid*, vol. 1, no. 1, pp. 20–27, Jun. 2010.

[11] *IEEE/IEC International Standard—Measuring Relays and Protection Equipment—Part 118-1: Synchrophasor for Power Systems—Measurements*, IEC/IEEE Standard 60255-118-1, 2018.

[12] Z. Huang, B. Kasztenny, V. Madani, K. Martin, S. Meliopoulos, D. Novosel, and J. Stenbakken, "Performance evaluation of phasor measurement systems," in *Proc. IEEE Power Energy Soc. Gen. Meeting-Convers. Del. Elect. Energy 21st Century*, Pittsburgh, PA, USA, Jul. 2008, pp. 1–7.

[13] A. P. S. Meliopoulos, F. Zhang, S. Zelingher, G. Stillman, G. J. Cokkinides, L. Coffeen, R. Burnett, and J. McBride, "Transmission level instrument transformers and transient event recorders characterization for harmonic measurements," *IEEE Trans. Power Del.*, vol. 8, no. 3, pp. 1507–1517, Jul. 1993.

[14] L. Zanni, D. Colangelo, R. Cherkaoui, and M. Paolone, "Impact of synchrophasor measurement types and uncertainties on the accuracy of distribution system linear state estimators," in *Proc. IEEE Eindhoven PowerTech*, Eindhoven, The Netherlands, Jun. 2015, pp. 1–6.

[15] S. Chakrabarti and E. Kyriakides, "PMU measurement uncertainty considerations in WLS state estimation," *IEEE Trans. Power Syst.*, vol. 24, no. 2, pp. 1062–1071, May 2009.

[16] M. Asprou, E. Kyriakides, and M. Albu, "The effect of parameter and measurement uncertainties on hybrid state estimation," in *Proc. IEEE Power Energy Soc. Gen. Meeting*, San Diego, CA, USA, Jul. 2012, pp. 1–8.

[17] J. Tang, J. Liu, F. Ponci, A. Monti, C. Muscas, and S. Sulis, "Impact of synchrophasor measurement uncertainty on detecting voltage stability margin in power systems," in *Proc. 3rd IEEE PES Innov. Smart Grid Technol. Eur. (ISGT Europe)*, Berlin, Germany, Oct. 2012, pp. 1–6.

[18] A. Perez, J. Møller, H. Jóhannsson, and J. Østergaard, "Uncertainty in real-time voltage stability assessment methods based on Thévenin equivalent due to PMU's accuracy," in *Proc. IEEE PES Innov. Smart Grid Technol., Eur.*, Istanbul, Turkey, Oct. 2014, pp. 1–6.

[19] T. Becejac, P. Dehghanian, and M. Kezunovic, "Impact of the errors in the PMU response on synchrophasor-based fault location algorithms," in *Proc. North Amer. Power Symp. (NAPS)*, Denver, CO, USA, Sep. 2016, pp. 1–6.

[20] C. Chen, J. Wang, and H. Zhu, "Effects of phasor measurement uncertainty on power line outage detection," *IEEE J. Sel. Topics Signal Process.*, vol. 8, no. 6, pp. 1127–1139, Jun. 2014.

[21] J. Zhao, A. Goldstein, and Y. Liu, "Model of parameterized PMU estimation error," in *Proc. IEEE Power Energy Soc. Gen. Meeting*, Chicago, IL, USA, Jul. 2017, pp. 1–5.

[22] G. Barchi, D. Macii, D. Belega, and D. Petri, "Performance of synchrophasor estimators in transient conditions: A comparative analysis," *IEEE Trans. Instrum. Meas.*, vol. 62, no. 9, pp. 2410–2418, Sep. 2013.

[23] J. Zhao, L. Zhan, Y. Liu, H. Qi, J. R. Gracia, and P. D. Ewing, "Measurement accuracy limitation analysis on synchrophasors," in *Proc. IEEE Power Energy Soc. Gen. Meeting*, Denver, CO, USA, Jul. 2015, pp. 1–5.

[24] A. P. S. Meliopoulos, G. J. Cokkinides, F. Galvan, and B. Fardanesh, "GPS-synchronized data acquisition: Technology assessment and research issues," in *Proc. Int. Conf. Syst. Sci.*, Kauia, HI, USA, Jan. 2006, p. 244c.

[25] A. S. Meliopoulos and G. J. Cokkinides, "Visualization and animation of instrumentation channel effects on DFR data accuracy," in *Proc. Georgia Tech Fault Disturbance Anal. Conf.*, Atlanta, GA, USA, 2002, pp. 1–7.

[26] A. P. Meliopoulos, V. Madani, D. Novosel, G. Cokkinides, R. Alaileh, B. Fardanesh, H. Huang, M. Ford, F. Mekic, U. Manmandhan, R. Hayes, J. Hackett, and S. Widergren, "Synchrophasor measurement accuracy characterization," North Amer. Synchrophasor Initiative Perform. Standards Task Team, Tech. Rep. NASPI-2007-TR-007, 2007. [Online]. Available: https://www.naspi.org/node/654/

[27] *American National Standard Requirements for Power-Line Carrier Coupling Capacitors and Coupling Capacitor Voltage Transformers (CCVT)*, Standard ANSI C93.1, 1999.

[28] *PMU Installation and Configuration Requirements, Version no. 1.0*, Mid-continent Independ. Syst. Operator, Carmel, IN, USA, 2012.

[29] *PMU Placement and Installation*, North Amer. Electr. Rel. Corp., Atlanta, GA, USA, 2016.

[30] *IEEE Guide for Synchronization, Calibration, Testing, and Installation of Phasor Measurement Units (PMUs) for Power System Protection and Control*, IEEE Standard C37.242-2013, 2013.

[31] R. M. Gardner, Z. Zhong, and Y. Liu, "Location determination of power system disturbances based on frequency responses of the system," U.S. Patent 7 519 454, Apr. 14, 2009.
[32] Y. Ye, "Wide-area situational awareness application developments," Ph.D. dissertation, Dept. Elect. Eng. Comput. Sci., Univ. Tennessee, Knoxville, Knoxville, TN, USA, 2011.
[33] P. Kundur, N. J. Balu, and M. G. Lauby, *Power System Stability and Control*, vol. 7. New York, NY, USA: McGraw-Hill, 1994.
[34] R. M. Gardner, "A Wide-area perspective on power system operation and dynamics," Ph.D. dissertation, Virginia Polytech. Inst. State Univ., Blacksburg, VA, USA, 2008.
[35] J. S. Thorp, C. E. Seyler, and A. G. Phadke, "Electromechanical wave propagation in large electric power systems," *IEEE Trans. Circuits Syst. I, Fundam. Theory Appl.*, vol. 45, no. 6, pp. 614–622, Jun. 1998.
[36] T. Funabashi, K. Koyanagi, and R. Yokoyama, "A review of islanding detection methods for distributed resources," in *Proc. IEEE Power Tech Conf.*, Bologna, Italy, Jun. 2003, pp. 1–6.
[37] J. Guo, Y. Zhang, M. A. Young, M. J. Till, A. Dimitrovski, Y. Liu, P. Williging, and Y. Liu, "Design and implementation of a real-time off-grid operation detection tool from a wide-area measurements perspective," *IEEE Trans. Smart Grid*, vol. 6, no. 4, pp. 2080–2087, Sep. 2014.
[38] A. Michiorri, H.-M. Nguyen, S. Alessandrini, J. B. Bremnes, S. Dierer, E. Ferrero, B.-E. Nygaard, P. Pinson, N. Thomaidis, and S. Uski, "Forecasting for dynamic line rating," *Renew. Sustain. Energy Rev.*, vol. 52, pp. 1713–1730, Dec. 2015.
[39] J. Zhao, J. Tan, L. Wu, L. Zhan, L. Yilu, J. R. Gracia, and P. D. Ewing, "Impact of measurement error on synchropahsor applications," Oak Ridge Nat. Lab., Oak Ridge, TN, USA, Tech. Rep. ORNL/TM-2015/314, 2015. [Online]. Available: http://www.osti.gov/servlets/purl/1212367/
[40] S. R. Júlíusson, "Using PMU measurements to assess dynamic line rating of transmission lines," M.S. thesis, Board Stud. Energy, Aalborg Univ., Aalborg, Denmark, 2013.
[41] *IEEE Standard for Calculating the Current-Temperature Relationship of Bare Overhead Conductors*, IEEE Standard 738-2012, 2013.
[42] S. G. Ghiocel, J. H. Chow, G. Stefopoulos, B. Fardanesh, D. Maragal, B. Blanchard, M. Razanousky, and D. B. Bertagnolli, "Phasor-measurement-based state estimation for synchrophasor data quality improvement and power transfer interface monitoring," *IEEE Trans. Power Syst.*, vol. 29, no. 2, pp. 881–888, Mar. 2014.

JIECHENG ZHAO (S'15–M'19) received the B.S. degree in automatic control from the Huazhong University of Science and Technology, Wuhan, China, in 2008, the Ph.D. degree in radio physics from the University of Chinese Academy of Sciences, Beijing, China, in 2013, and the Ph.D. degree in power system from The University of Tennessee, Knoxville, TN, USA.

He is currently a Senior Engineer with Dominion Energy, Richmond, VA, USA. His research interests include power system monitoring, PMU applications, DER integration, microgrid, and power system protection.

JIN TAN (S'11–M'15) received the B.E. and Ph.D. degrees in electrical engineering from Southwest Jiaotong University, Chengdu, China, in 2007 and 2014, respectively.

From 2009 to 2011, she was a visiting Ph.D. student with the Department of Energy Technology, Aalborg University, Denmark. In 2014, she was a Postdoctoral Researcher with the Department of Electrical Engineering and Computer Science, The University of Tennessee, Knoxville, TN, USA. In January 2015, she joined the National Renewable Energy Laboratory (NREL), Golden, CO, USA, where she is currently a Senior Engineer with the Power Systems Engineering Center. Her research interests include power system stability with large-scale renewable integration, multitimescale dynamic modeling of various renewable generation, ancillary control of renewable integration, and energy storage for grid applications.

Dr. Tan is a member of Power and Energy Society (PES) and IEEE Women in Engineering. She received President Award from the National Renewable Energy Laboratory, in 2018. She is the Editor of *International Transaction on Electrical Energy System*.

LING WU (S'15–M'19) received the B.S. and M.S. degrees in electrical engineering from Xi'an Jiaotong University, in 2008 and 2011, respectively, and the Ph.D. degree in electrical engineering from The University of Tennessee, Knoxville, in 2017.

She is currently with the Schneider Electric Andover Research and Development Center, Andover, MA, USA. Her research interests include data mining, embedded systems, the Internet of Thing, and edge computing.

LINGWEI ZHAN (S'13–M'15) received the B.S. and M.S. degrees in electrical engineering from Tongji University, in 2008 and 2011, respectively, and the Ph.D. degree from the Department of Electrical Engineering and Computer Science, The University of Tennessee, Knoxville, in 2015.

He is currently a Research and Development staff with the Oak Ridge National Laboratory. His research interests include advanced grid monitors, PMU, synchrophasor measurement algorithms, wide-area power system monitoring, renewable energy sources, FACTs, and HVDC.

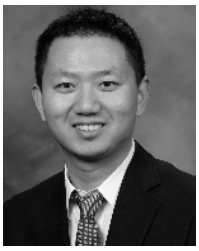

WENXUAN YAO (S'15–M'19) received the B.S. and Ph.D. degrees from the College of Electrical and Information Engineering, Hunan University, Changsha, China, in 2011 and 2017, respectively, and the Ph.D. degree from the Department of Electrical Engineering and Computer Science, the University of Tennessee, Knoxville, USA, in 2018.

He is currently a Research Associate with the Oak Ridge National Laboratory. His research interests include wide-area power system monitoring, synchrophasor measurement application, embedded system development, power quality diagnosis, and big data analysis in power systems.

YILU LIU (S'88–M'89–SM'99–F'04) received the B.S. degree from Xian Jiaotong University, China, and the M.S. and Ph.D. degrees from Ohio State University, Columbus, in 1986 and 1989, respectively.

She was a Professor with Virginia Tech, where she led the effort to create the North American power grid frequency monitoring network, which is currently operated with The University of Tennessee, Knoxville (UTK), and the Oak Ridge National Laboratory (ORNL) as GridEye. She is also the Governor's Chair with UTK and ORNL. She is also the Deputy Director of the DOE/NSF-cofunded Engineering Research Center CURENT. Her current research interests include power system wide-area monitoring and control, large interconnection-level dynamic simulations, electromagnetic transient analysis, and power transformer modeling and diagnosis. She is a member of the U.S. National Academy of Engineering and the National Academy of Inventors.